Science of the Total Environment 773 (2021) 145546

Contents lists available at ScienceDirect

Science of the Total Environment

journal homepage: www.elsevier.com/locate/scitotenv

Transformation of jarosite during simulated remediation of a sandy sulfuric soil

Angelika Kölbl [a,*], Klaus Kaiser [a], Pauline Winkler [a], Luke Mosley [b], Rob Fitzpatrick [b], Petra Marschner [c], Friedrich E. Wagner [d], Werner Häusler [e], Robert Mikutta [a]

[a] Soil Science and Soil Protection, Martin Luther University Halle-Wittenberg, 06120 Halle (Saale), Germany
[b] Acid Sulfate Soils Centre, The University of Adelaide, South Australia 5064, Australia
[c] School of Agriculture, Food and Wine, The University of Adelaide, South Australia 5005, Australia
[d] Physik Department, Technische Universität München, 85747 Garching, Germany
[e] Lehrstuhl für Bodenkunde, Technische Universität München, 85350 Freising, Germany

HIGHLIGHTS

- Straw supply induced reduction processes and pH increase in submerged sulfuric soils.
- Both reducing conditions and pH increase contributed to dissolution of jarosite.
- Fe^{3+} was partly reduced but SO_4^{2-} reduction was little during 15-week incubation.
- No sulfides, but Fe^{III} oxyhydroxides and Fe^{2+}/Fe^{3+}–organic matter associates formed.
- Prior pH adjustment is not necessary for remediation of a sandy sulfuric soil.

GRAPHICAL ABSTRACT

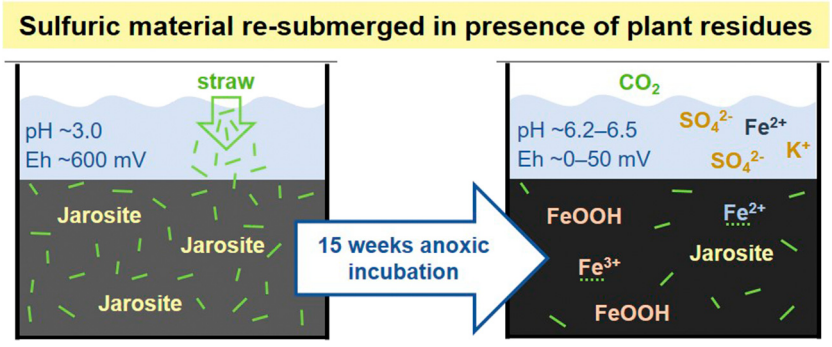

ARTICLE INFO

Article history:
Received 10 December 2020
Received in revised form 23 January 2021
Accepted 27 January 2021
Available online 3 February 2021

Editor: Filip M.G.Tack

Keywords:
Acid sulfate soil
Anoxic incubation
Organic matter addition
Fe-oxyhydroxides
Fe^{2+}/Fe^{3+}–organic matter associates

ABSTRACT

Aeration of wetland soils containing iron (Fe) sulfides can cause strong acidification due to the generation of large amounts of sulfuric acid and formation of Fe oxyhydroxy sulfate phases such as jarosite. Remediation by re-establishment of anoxic conditions promotes jarosite transformation to Fe oxyhydroxides and/or Fe sulfides, but the driving conditions and mechanisms are largely unresolved. We investigated a sandy, jarosite-containing soil (initial pH = 3.0, Eh ~600 mV) in a laboratory incubation experiment under submerged conditions, either with or without wheat straw addition. Additionally, a model soil composed of synthesized jarosite mixed with quartz sand was used. Eh and pH values were monitored weekly. Solution concentrations of total dissolved organic carbon, Fe, S, and K as well as proportions of Fe^{2+} and SO_4^{2-} were analysed at the end of the experiment. Sequential Fe extraction, X-ray diffraction, and Mössbauer spectroscopy were used to characterize the mineral composition of the soils. Only when straw was added to natural and artificial sulfuric soils, the pH increased up to 6.5, and Eh decreased to approx. 0 mV. The release of Fe (mainly Fe^{2+}), K, and S (mainly SO_4^{2-}) into the soil solution indicated redox- and pH-induced dissolution of jarosite. Mineralogical analyses confirmed jarosite losses in both soils. While lepidocrocite formed in the natural sulfuric soil, goethite was formed in the artificial sulfuric soil. Both soils showed also increases in non-sulfidized, probably organically associated Fe^{2+}/Fe^{3+}, but no (re-)formation of Fe sulfides. Unlike Fe sulfides, the formed Fe oxyhydroxides are not prone

* Corresponding author.
E-mail address: angelika.koelbl@landw.uni-halle.de (A. Kölbl).

https://doi.org/10.1016/j.scitotenv.2021.145546

to support re-acidification in the case of future aeration. Thus, inducing moderately reductive conditions by controlled supply of organic matter could be a promising way for remediation of soils and sediments acidified by oxidation of sulfuric materials.

1. Introduction

Wetland soils containing Fe sulfides are productive ecosystems but pose a major threat to the environment when they fall dry, as for example after drainage or during drought periods (Fanning et al., 2017; Stirling et al., 2020). They are wide-spread throughout the world in coastal and inland areas, e.g. in southern Australia (Fanning et al., 2017). Upon aeration, oxidation of Fe sulfides (principally pyrite) causes strong acidification when insufficient acid neutralising capacity is present, the resulting soils are commonly referred to as acid sulfate soils with sulfuric material (pH <4) or sulfuric soils (Fitzpatrick, 2013). Some of the major environmental hazards associated with acidification of soils and waters are aluminium toxicity, trace metal/metalloid mobilization, and de-vegetation. Acidification can even result in the corrosion of concrete and steel infrastructure (see Karimian et al., 2018a, and references therein). Oxidation of pyrite and subsequent acidification is often accompanied by the formation of pale yellow masses of jarosite ($KFe_3(SO_4)_2(OH)_6$), a common mineral in sulfuric soils and acidic, sulfate-rich environments (Baron and Palmer, 1996). Jarosite is a barrier to sulfuric soil remediation as it is only sparingly soluble and buffers the soil at a pH of approximately 3.5 (e.g. Trueman et al., 2020). Jarosite can incorporate various elements into its structure during formation, and is an important scavenger for arsenic, antimony, chromium, and lead in acid sulfate soils as well as environments affected by acid mine drainage (Karimian et al., 2017; Johnston et al., 2012; Welch et al., 2007).

A common approach to remediate sulfuric soils is re-submergence (e.g. Fanning et al., 2017). After saturation and the re-establishment of reducing conditions, sulfate-reducing bacteria (SRB) can induce re-formation of Fe sulfide minerals (e.g. Johnston et al., 2009). Many of these microorganisms are heterotrophic and require organic carbon (OC) for growth and metabolism (Berner, 1984; Plugge et al., 2011). Low pH (<4.5) can limit the activity of SRB, even after organic matter (OM) addition (Yuan et al., 2015a). Therefore, the activity of SRB is often limited by both: low pH and low availability of OC. The activity of SRB can be promoted by proton consumption induced by Fe-reducing bacteria (dos Santos Afonso and Stumm, 1992). Dissimilatory Fe reduction can occur at low pH and is carried out by many types of bacteria, using a wide range of electron donors. Naturally occurring OM acts as electron donor for Fe-reducing bacteria (Lovley, 1995). Once the pH increases to more favourable levels (4.5–5), SRB communities become active and can further increase the pH (Coggon et al., 2012). Thus, the addition of plant residues can activate a sequence of reducing bacteria, resulting in a pH increase up to circumneutral levels during submerged periods (Yuan et al., 2015a, 2015b; Jayalath et al., 2016a, 2016b; Kölbl et al., 2018). Pre-adjustment of the pH to values ≥4.5 can accelerate soil remediation (e.g. Yuan et al., 2015a; Kölbl et al., 2018).

Large additions of undecomposed plant residues with high proportions of polysaccharides has been shown to induce fast reduction processes, and thus, rapid remediation of clayey as well as sandy sulfuric soils (Kölbl et al., 2018, 2019). However, it is not well established as to what extent the OC-mediated reduction causes dissolution of the Fe oxyhydroxy sulfates, such as jarosite, which is formed during previous aeration events. Jarosite is only stable between pH 3 and 4 (Zahrai et al., 2013) and under sufficiently oxic conditions (Eh >400 mV; Keene et al., 2010). A drop in Eh to a critical level and a concomitant pH increase, e.g. due to activity of reducing bacteria in the presence of available OM, may cause the dissolution of jarosite. It has been shown that increasing amounts of added OM can induce jarosite dissolution, resulting in increased solution concentrations of Fe and sulfate under inundation (Chu et al., 2006). The presence of organic ligands has also been shown to enhance the dissolution of jarosite (Trueman et al., 2020). However, dissolution of jarosite may have unintended and undesirable consequences, releasing acid and potentially toxic trace metals into the environment (Welch et al., 2007).

Some studies investigated products of jarosite dissolution. The Fe oxyhydroxides goethite (α-FeOOH) and lepidocrocite (γ-FeOOH) have been identified as products of Fe^{II}-catalysed transformation (e.g. Jones et al., 2009; Vithana et al., 2015; Bao et al., 2018), whereas mackinawite (Fe^{II} sulfide) formed as mineral end product of jarosite sulfidization (Johnston et al., 2012). Thus, to the best of our knowledge, the transformation of jarosite to Fe oxyhydroxides and/or Fe sulfides under reducing conditions induced by OM addition remains largely unresolved. This is crucial for successful remediation of jarosite-containing soils since the type of transformation products strongly affects potential acidification and mobility of trace metals and metalloids. Well-defined laboratory experiments addressing the mechanisms and conditions driving jarosite transformation can help to fill the knowledge gap.

The objective of this study was to track the fate of jarosite during simulated remediation of a sandy acid sulfate soil with sulfuric material in anoxic laboratory incubation experiments with detailed monitoring of pH and redox conditions. We also used a synthesized jarosite mixed with quartz sand as mineralogically well-defined model of the natural sulfuric soil, allowing for precise tracking of jarosite-derived Fe without interference of other co-occurring Fe-bearing minerals. This enables an unbiased view to the transformation of jarosite under submerged condition with OM addition. Particular attention was paid to the dissolution of jarosite and the potential (re-)formation of Fe sulfides after establishing anoxic conditions. We assume that the supply of sufficient available OM induces: (i) dissolution of jarosite due to reductive dissolution and pH increase, (ii) Eh values low enough to reduce both the released Fe^{3+} and sulfate, and (iii) the (re-)formation of Fe sulfides. In addition, we assume that (iv) the pre-adjustment of the pH to values ≥4.5 will accelerate jarosite dissolution and sulfide formation.

2. Materials and methods

2.1. Sampling area

Samples of a sandy acid sulfate soil with sulfuric material were collected in November 2017 from the Gillman site in the Barker Inlet estuary (sandy marine deposits) close to Adelaide (South Australia). The Gillman site is a former tidal wetland, which was covered with mangrove woodland (Fitzpatrick et al., 2012). The Gillman area was reclaimed from intertidal and supratidal areas in 1935 when a series of bund walls were constructed. The loss of tidal inundation caused lowering of the water table, and subsequent oxygen diffusion into hypersulfidic material, which induced pyrite oxidation, resulting in pH values ≤3 and the formation of sulfuric material (Poch et al., 2009; Fitzpatrick et al., 2012; Michael et al., 2015). Pale yellow jarosite mottles formed along relict mangrove roots and pneumatophore channels. The soil was classified as sulfuric soil in accordance with the Australian acid sulfate soil classification (Fitzpatrick, 2013). According to the Australian Soil Classification (Isbell and National Committee on Soils and Terrain, 2016), the soil was classified as Peaty, Sulfuric, Hypersalic Hydrosol, and as Salic Fluvisol (Hyperthionic, Drainic) according to WRB identification keys (IUSS Working Group WRB, 2015).

Soil material was taken from a sandy soil horizon (pH_{H2O} = 3.0) at 80–100 cm depth in a pit. We selected the deep subsoil layer in order to avoid inputs of high amounts of fresh OM, and thus, allowing for studying exclusively the impact of added OM sources. The soil material was immediately dried in a fan-forced oven at 60 °C to suppress microbial activity, sieved to <2 mm, and then shipped to Germany for analysis. Basic soil properties are given in Table 1.

2.2. Synthesis of jarosite and preparation of an artificial sandy sulfuric soil

Potassium-jarosite was synthesized according to a slightly modified method of Driscoll and Leinz (2005). Briefly, 25.8 g $Fe_2(SO_4)_3 \cdot nH_2O$ (Alfa Aesar, Germany) was dissolved in a 250-ml glass bottle containing 130 ml H_2O_{dest}. Next, 18.7 g of 45 wt% KOH solution (Sigma Aldrich, Germany) was added. The glass bottle was tightly closed and the solution mixed thoroughly by hand shaking. The solution was placed in a furnace and heated for 5 h at 140 °C. After cooling to room temperature, the liquid phase was decanted and the precipitated K-jarosite was washed twice by H_2O_{dest} adjusted to pH 3 by HCl. After drying overnight in an oven at 60 °C, the solid K-jarosite was weighed and stored dry for further analyses.

Assuming that almost all Fe (total Fe, Table 1) of the natural sulfuric soil can be attributed to jarosite, we prepared an artificial sulfuric soil by mixing synthesized jarosite with quartz sand. We used 0.915 g g^{-1} quartz sand (0.1–0.315 μm, p.a., Carl Roth, Germany) and 0.060 g g^{-1} quartz powder (<0.063 μm, Carl Roth, Germany) to simulate the texture of the natural soil, and added 0.025 g g^{-1} synthesized jarosite. Assuming a share of Fe of 33.45 weight-% in the synthesized jarosite ($KFe_3(SO_4)_2(OH)_6$), the resulting total Fe concentration of the soil mixture was 8.36 mg g^{-1}. The artificial soil had properties similar to those of the natural sulfuric soil (except for the OC concentration, Table 1). The sulfuric soils are henceforth referred to as "natural soil" and "artificial soil".

2.3. Incubation experiments

Samples of the natural and artificial sulfuric soil were prepared by placing 25 g of dry mass into 250 ml incubation bottles. All samples were adjusted to field capacity (determined in pre-experiments) and pre-incubated for two weeks at 20 °C under oxic conditions to re-establish conditions similar to those in the field. The bottles were aerated weekly, and pH and Eh (combined pH and redox electrode, Hach Lange GmbH, Germany) were determined. After two weeks of oxic pre-incubation, the natural soil samples were submerged by adding 50 ml of degassed H_2O_{dest} under Ar atmosphere in an airtight glovebox (pO_2 ≤2%). Then, one set of samples received 320 mg ground wheat straw (OC: 450 mg g^{-1}, N: 2.5 mg g^{-1}; details and chemical composition of OM are given in Kölbl et al. (2019)), while another set was incubated without wheat straw. Half of the samples with and without straw addition were adjusted to pH 5.2 using 0.1 M NaOH to establish optimal conditions for SRB (Yuan et al., 2015a, 2015b) and to test if pH pre-adjustment can be used to accelerate Fe- and sulfate-reduction processes. The other half of the samples was incubated without pH adjustment.

The anoxic incubation of the artificial soil was set up the same way, except for adding soil solution derived from the natural soil instead of degassed H_2O_{dest}, to obtain a similar solution as for the natural soil. The soil solution was prepared by adding degassed H_2O_{dest} to the natural soil at the same soil-to-solution ratio as in the incubation experiment. After one week of anoxic incubation and settling of the soil particles, the supernatant was sucked off in the glovebox, shaken, and added to the artificial soil samples at 50 ml portions. An aliquot of the soil solution was frozen at −20 °C for further analyses.

All anoxic incubations were conducted in the dark at 20 °C for 15 weeks. The treatments had four replicates; the initial OC concentrations are summarized in Table 2. Once a week, samples were shaken and suspensions analysed for pH and Eh under Ar atmosphere as described above. At the end of the experiment, the suspensions were transferred into airtight centrifugation bottles and centrifuged for 10 min at 3000*g*. The supernatants were filtered in the glovebox through 0.45-μm polyethersulfone membranes (Pall Corporation, USA), and then stored at −20 °C. The settled soil material was freeze-dried. After freeze-drying, one out of four replicates was divided into two distinct fractions: the dark and fine (organo-rich) mineral layer settled on top was carefully separated from the quartz-dominated bottom layer. This separation was done to obtain a fine fraction enriched in Fe oxyhydroxides, Fe oxyhydroxy sulfates or Fe sulfides but low in quartz. All soil samples were stored in airtight vessels under Ar atmosphere prior to analysis.

2.4. Elemental analysis of soil solution

Total concentrations of Fe, K, and S in the supernatants were measured by inductively coupled plasma optical emission spectroscopy (ICP-OES) (Ultima 2, Horiba Ltd., Japan). Prior to the measurements, the samples were acidified to pH <2 using 0.1 M HCl. Sulfate (SO_4^{2-}) was measured with an ion chromatograph (DX120, Dionex Corporation, USA), using an IonPac AS22 column. Dissolved Fe^{2+} was determined by reaction with ferrozine (modified after Stookey, 1970) in the glovebox and subsequent photometric detection at 562 nm (Specord 210 plus, Analytik Jena AG, Germany). Dissolved organic carbon (DOC) was measured with a TOC-analyser (Multi N/C 3100, Analytik Jena AG, Germany) after acidification to pH <2 with 0.1 M HCl. Saturation indices for Fe oxyhydroxides, Fe oxyhydroxy sulfates, and Fe sulfides were estimated from element concentrations and pH/Eh properties of the soil solution using Visual MINTEQ 3.1 (https://vminteq.lwr.kth.se).

2.5. Characterization of sulfuric soils before and after incubation

All bulk soil samples were analysed for OC by dry combustion at 950 °C using a Vario MAX cube elemental analyser (Elementar Analysensysteme GmbH, Germany).

A modified version of the sequential wet chemical extraction procedure suggested by Claff et al. (2010) was used to estimate several Fe fractions in bulk natural and artificial soil samples: (1) exchangeable (magnesium chloride-extractable), (2) acid-soluble (hydrochloric acid), (3) crystalline oxide (dithionite-citrate-bicarbonate-extractable; DCB), and (4) pyrite-bound (nitric acid-extractable) Fe. During the

Table 1
Basic properties of the natural and artificial sulfuric soil (SD: standard deviation).

Sulfuric soil	pH_{water}	OC		N		Total Fe		Total S		Sand	Silt	clay
		mg g^{-1}		mg g^{-1}		mg g^{-1}		mg g^{-1}		%	%	%
		Mean	SD	Mean	SD	Mean	SD	Mean	SD			
Natural	3.0	3.57	0.19	0.22	0.04	8.31[a]	0.16	3.05[a]	0.02	92	6	2
Artificial	3.3	0.90[b]	0.10	0.22[b]	0.01	8.36[c]		3.20[c]		92	7	1

[a] Analysed by digestion with $HF/HClO_4$ and subsequent Fe analysis with ICP-OES.
[b] OC and N concentration due to added soil solution: OC: 17.9 mg l^{-1}; N: 4.4 mg l^{-1}.
[c] Total Fe and S concentration calculated from addition of synthesized jarosite.

Table 2
Soil organic carbon (OC) concentrations of natural and artificial soil treatments as well as respective dissolved OC (DOC) concentrations before and after incubation (mean values and standard deviation (SD) of four replicates). Different letters indicate significantly different mean values between treatments ($p < 0.05$). OC values for treatments with wheat straw addition before incubation were calculated (initial OC + amount of added OC) and therefore have no standard deviation.

	Before incubation				After incubation			
	Soil OC mg g^{-1} soil		DOC mg l^{-1}		Soil OC mg g^{-1} soil		DOC mg l^{-1}	
	Mean	SD	Mean	SD	Mean	SD	Mean	SD
Natural soil								
No straw	3.57	0.19	-		3.31[b]	0.08	16.6[b]	0.9
No Straw + pH adjustment	3.57	0.19	-		3.34[b]	0.57	22.3[b]	3.2
+ Straw*	9.33		-		8.22[a]	0.40	42.4[a]	3.0
+ straw* + pH adjustment	9.33		-		7.53[a]	1.06	39.8[a]	3.6
Artificial soil								
No straw**	-		17.9[a]	0.5	0.10[b]	0.01	4.7[c]	0.2
No straw**+ pH adjustment	-		17.9[a]	0.5	0.10[b]	0.02	4.3[c]	0.4
+ Straw*	5.76		17.9[a]	0.5	4.94[a]	0.23	63.9[a]	17.9
+ Straw* + pH adjustment	5.76		17.9[a]	0.5	5.19[a]	0.17	30.5[b]	3.5

* OC and N concentrations of added wheat straw: OC: 450 mg g^{-1}, N: 2.5 mg g^{-1}; details and chemical composition of organic matter are given in Kölbl et al. (2019).
** OC and N concentration due to added soil solution: OC: 17.9 mg l^{-1}, N: 4.4 mg l^{-1}.

first step, 2 g soil material was extracted by shaking in 40 ml 1 M $MgCl_2$ solution for 1 h in a reciprocating shaker. After centrifugation (10 min, 3000 *g*), the supernatant was filtered through 0.45-μm syringe filters (PTFE membrane filters, VWR International, Belgium). Thereafter, 40 ml 1 M HCl was added to the settled soil material and the sample shaken for 4 h; the supernatant was extracted as described before. The subsequent DCB extraction was carried out as outlined by Mehra and Jackson (1960). Finally, 40 ml of 65% HNO_3 was added, the samples shaken for 2 h, and then, the supernatant was extracted as described above. Concentrations of extracted Fe were determined by ICP-OES.

The mineral composition of one fine fraction of each treatment was analysed on random powder samples using X-ray diffraction (XRD) (D5005, Siemens AG, Germany) with Cu Kα-radiation ($\lambda = 1.541$ nm) from 2 to 80°2θ in stepscan mode with 0.02°2θ-step size, fixed slits, and 10 s counting time. We presented the range from 10 to 80°2Θ which cover the signals of jarosite.

Mössbauer spectra of selected fine fractions after incubation with and without straw addition were used to identify all Fe-containing compounds. Samples were measured in transmission geometry with a standard electromechanical spectrometer using a sinusoidal velocity waveform and a 25 mCi source of ^{57}Co in rhodium. The 14.4-keV γ-rays were detected with a Kr/CO_2 proportional counter with single channel analyser windows set on both the 14.4 keV photo peak and the escape peak. In addition to the measurements at room temperature (295 K), spectra were recorded at 4.2 K in a liquid He bath cryostat, and measurements at about 150 K were performed with liquid nitrogen in the heat radiation shield of the cryostat. During all measurements, source and absorber were at the same temperature. The absorber thickness was 150 mg cm^{-2} for all samples. The spectra were least squares fitted with appropriate superpositions of Lorentzian lines for quadrupole doublets and magnetically split sextets. In some cases, broad magnetic patterns were approximated by Gaussian distributions of hyperfine fields.

2.6. Statistical evaluation

Mean values between treatments were compared with ANOVA using a Tukey procedure as post-hoc test. For all statistical tests, a significance level of 0.05 was used. All statistical analyses were carried out using OriginPro 2019 (OriginLab Corporation, USA).

3. Results

3.1. pH and Eh

During the 14 days of oxic pre-incubation, pH values remained constant at ~3.1 (natural soil), or increased slightly from 3.3 to 3.6 (artificial soil). The Eh values varied between 580 and 600 mV for the natural soil, and were constant at ~650 mV for the artificial soil (Fig. 1).

After submergence, the treatments developed different pH and Eh values. Addition of wheat straw induced a pH increase to 6.2 in artificial and 6.5 in natural soil samples at the end of the incubation. Adjustment of pH at the beginning of the anoxic phase accelerated the pH increase but resulted in similar final pH values. The Eh values decreased after wheat straw addition, reaching ~0 (natural soil) and 50 mV (artificial soil) at the end of the incubation, irrespective of the pH adjustment. Natural and artificial soils without straw addition had pH values of 3.5 and 4.0 and Eh values of 600 and 500 mV at the end of the incubation, respectively. Adjustment of pH in samples without wheat straw addition resulted in slightly higher pH (~4.5) but similar Eh values (500–600 mV) compared to non pH-adjusted samples.

3.2. Soil OC before and after incubation

In natural soil samples without wheat straw addition, the OC concentration decreased slightly from 3.6 to 3.3 mg g^{-1} after incubation (Table 2), irrespective the pH adjustment. In natural soil samples with straw addition, OC concentrations decreased from 9.3 to 8.2 mg g^{-1} without pH adjustment and to 7.5 mg g^{-1} with pH adjustment.

In the artificial soil, DOC equivalent to 0.9 mg OC g^{-1} was added with the soil solution. Without straw addition, the soil OC concentration was 0.1 mg g^{-1} after incubation. With straw addition, soil OC concentrations decreased from ~5.8 to ~4.9 mg g^{-1}, irrespective the pH adjustment.

3.3. Soil solution composition

Concentrations of DOC at the end of the incubations ranged from 4 to 64 mg l^{-1} (Table 2). Lowest values were found in solutions without straw addition (in artificial soil samples up to 5 mg l^{-1} and in natural soil samples up to 22 mg l^{-1}). The DOC concentrations in treatments with straw addition were significantly higher and ranged between 31 and 64 mg l^{-1}.

In treatments without straw addition, total Fe concentrations in the soil solution were low (maximum values of 0.04 mmol l^{-1}, Table 3). In treatments with straw addition, Fe concentrations after anoxic incubation were higher, ranging from ~11.9 mmol l^{-1} (artificial soil) to 12.9 mmol l^{-1} (natural soil). Due to their large variability, Fe concentrations were not significantly different between natural and artificial soils. The proportion of Fe^{2+} was ≥97% of the total Fe concentrations in all soil solutions. Adjustment of pH at the beginning of the submerged incubation had only minor effects on the Fe release.

The initial K concentration in the soil solution was 0.8 mmol l^{-1} and did not change significantly after incubation of treatments without straw addition. In treatments with straw addition, K concentrations increased, ranging from 10 mmol l l^{-1} (natural soil) to 13 mmol l^{-1} (artificial soil), with 2.4 mmol l^{-1} being straw-derived. Pre-adjustment of pH at the beginning of the anoxic incubation had no effect on dissolved K concentrations.

Total S concentrations did also not change significantly after incubation of samples without straw addition, ranging from 3 mmol l^{-1} (artificial soil) to 5 mmol l^{-1} (natural soil). Incubation with straw addition resulted in increased S concentrations of 21 mmol l^{-1} in artificial and 23 mmol l^{-1} in natural soil. The share of SO_4^{2-}-S was 70% of the total dissolved S in the artificial and 80% in the natural soil. Adjustment of pH had also no significant effect on dissolved S concentrations.

Congruent dissolution of jarosite ($KFe_3(SO_4)_2(OH)_6$) should lead to a stoichiometric Fe:K:S molar ratio of 3:1:2 in solution. Addition of wheat

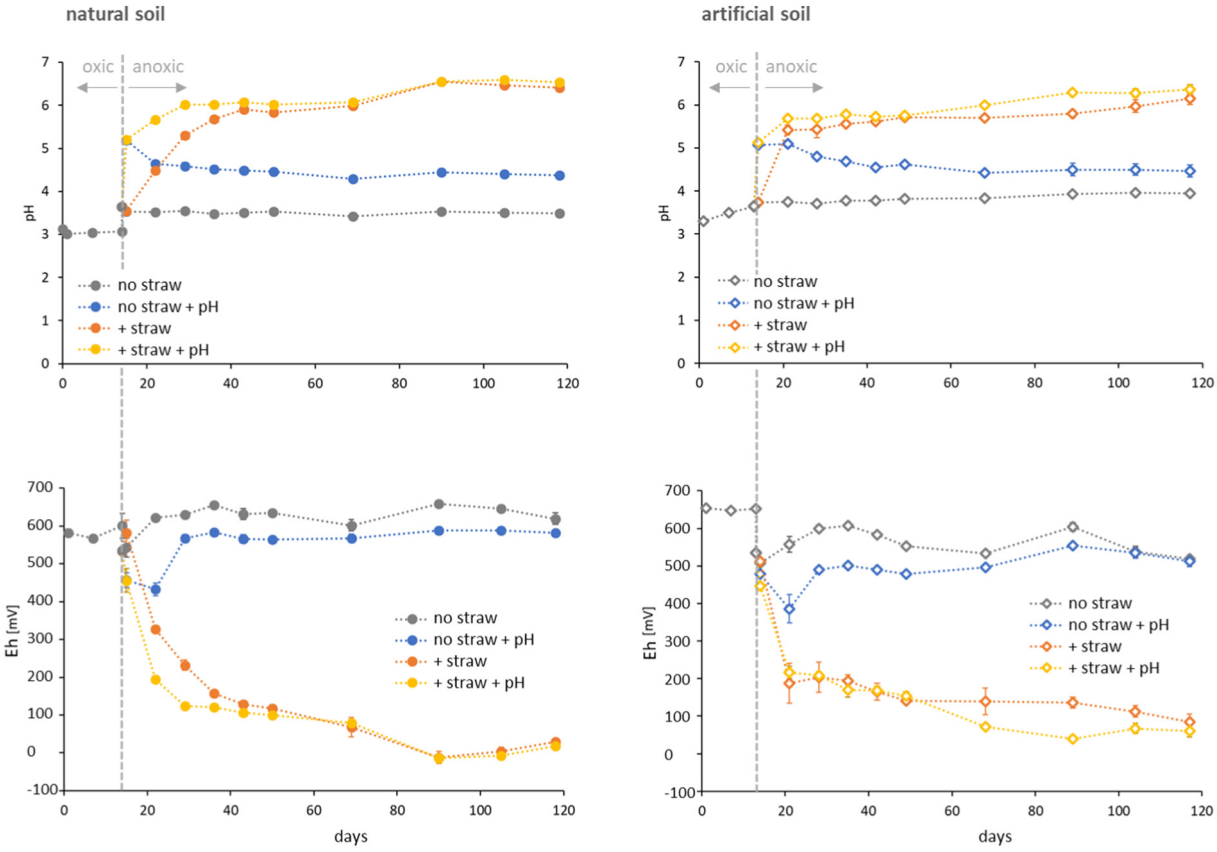

Fig. 1. Time course of pH and Eh values in natural and artificial soil during the incubation experiment. Data points show mean values ± standard deviations ($n = 4$).

straw added K but no Fe and S to the soil solution (Table 3). Therefore, the portion of straw-derived K was subtracted before calculating element ratios in solution. The calculated average molar Fe:K:S ratios in solution after incubation with straw, being 1.6:1:2.6 for the natural soil and 1.2:1:2.1 for the artificial soil, did not accord with those expected for congruent dissolution of jarosite.

3.4. Fe species before and after incubation

X-ray diffraction patterns of natural and artificial soils clearly revealed the occurrence of jarosite before incubation (Fig. 2). Incubation without straw addition did not affect the presence of jarosite. After incubation with wheat straw, jarosite was no longer detectable by XRD in the natural soil. In the artificial soil with straw addition, however, jarosite was still detectable by XRD after incubation (Fig. 2).

The sequential extraction of natural and artificial soils before incubation revealed that most Fe was DCB-extractable, with 4.0 mg g^{-1} in the natural soil and 4.9 mg g^{-1} in the artificial soil (Fig. 3). Hydrochloric acid extracted 1.4 mg Fe g^{-1} from the natural and 1.9 mg Fe g^{-1} from the artificial soil. All other extraction steps revealed very low Fe contents (≤0.1 mg g^{-1}). Incubation without straw did not change the distribution of Fe over fractions significantly. After incubation with straw, DCB-extractable Fe was reduced by 57% in the natural soil and by 26% in the artificial soil, whereas HCl-extractable Fe increased by 1.0 mg g^{-1} in natural and 0.4 mg g^{-1} in artificial soil. In addition, ~1.4 mg g^{-1} of Fe was in the soil solution in the natural soil as well as artificial soil.

Table 3
Concentrations of Fe, Fe^{2+}, K, S, and SO_4^{2-} in solutions of natural and artificial soil treatments at the start (after 1 week of anoxic incubation) and at the end of the incubation experiment (mean values and standard deviation (SD) of four replicates). Different letters indicate significantly different mean values between treatments ($p < 0.05$).

		Natural soil					Artificial soil				
		Fe	Fe^{2+}	K	S	SO_4^{2-}	Fe	Fe^{2+}	K	S	SO_4^{2-}
		mmol l^{-1}	mmol l^{-1}	mmol l^{-1}	mmol l^{-1}	mmol l^{-1}	mmol l^{-1}	mmol l^{-1}	mmol l^{-1}	mmol l^{-1}	mmol l^{-1}
Start of incubation											
No Straw	**mean**	**0.01^{c}**	**0.01^{c}**	**0.81^{b}**	**2.66^{b}**	**1.02^{b}**	**0.01^{b}**	**0.01^{b}**	**0.81^{b}**	**2.66^{b}**	**1.02^{b}**
	SD	0.01	0.01	0.13	0.34	8.39	0.01	0.01	0.13	0.34	8.39
End of incubation											
no straw	**mean**	**0.00^{c}**	**0.00^{c}**	**1.00^{b}**	**4.68^{b}**	**3.78^{b}**	**0.00^{b}**	**0.04^{b}**	**1.06^{b}**	**2.61^{b}**	**1.78^{b}**
	SD	0.00	0.00	0.24	0.25	0.20	0.00	0.04	0.32	0.17	0.10
no straw + pH	**mean**	**0.00^{c}**	**0.01^{c}**	**0.73^{b}**	**4.99^{b}**	**3.63^{b}**	**0.00^{b}**	**0.00^{b}**	**1.11^{b}**	**3.06^{b}**	**2.01^{b}**
	SD	0.00	0.01	0.25	0.13	0.53	0.00	0.00	0.29	0.27	0.19
+ straw	**mean**	**12.85^{a}**	**12.42^{a}**	**9.97^{a}**	**23.17^{a}**	**17.89^{a}**	**11.85^{a}**	**11.66^{a}**	**10.87^{a}**	**19.47^{a}**	**14.25^{a}**
	SD	0.71	0.45	0.68	1.84	2.27	2.22	2.14	1.37	2.71	2.39
+ straw + pH	**mean**	**11.57^{b}**	**11.50^{b}**	**9.94^{a}**	**21.67^{a}**	**18.67^{a}**	**11.33^{a}**	**11.17^{a}**	**12.94^{a}**	**21.35^{a}**	**15.95^{a}**
	SD	0.20	0.56	0.37	0.38	1.39	2.83	2.51	1.41	3.76	2.09
Straw-derived	**mean**	**0.00**	**0.00**	**2.44**	**0.00**	**0.00**	**0.00**	**0.00**	**2.44**	**0.00**	**0.00**
	SD	0.00	0.00	0.00	0.00	0.00	0.00	0.00	0.00	0.00	0.00

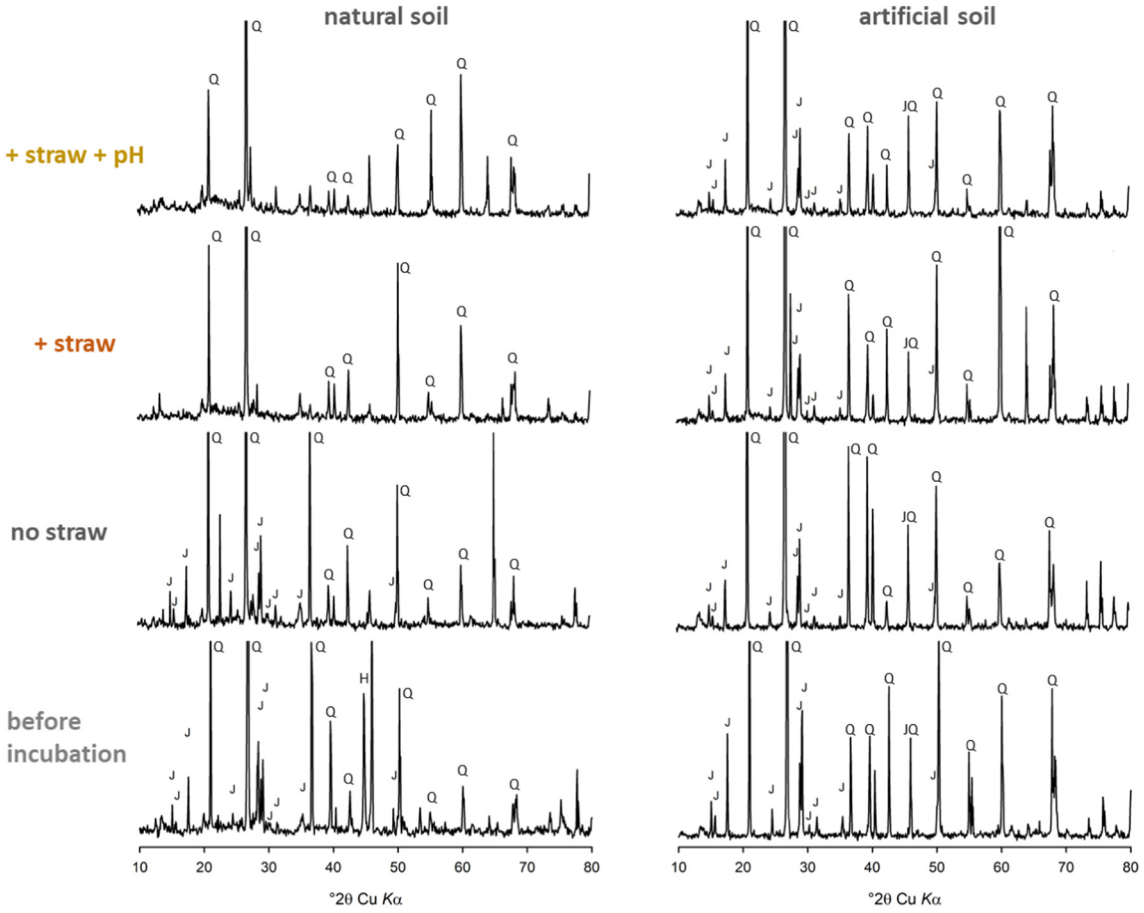

Fig. 2. Powder XRD patterns of natural and artificial soil treatments (fine fractions) before and after incubation (J = jarosite; Q = quartz; H = halite).

Adjustment of pH before incubation had no significant effect on the distribution of Fe fractions.

The identification of different Fe phases with Mössbauer spectroscopy is carried out by measuring the same sample at different temperatures. Most Fe minerals that occur in soils (e.g. haematite, goethite, jarosite) are represented in the Mössbauer spectrum by a doublet or they magnetically order into a sextet. Highly crystalline Fe^{III} minerals form a sextet already at room temperature, while less crystalline Fe^{III} minerals require lower measurement temperatures. Those Fe^{III} minerals that have not ordered at a certain measurement temperature collectively form a ferric doublet of unresolved Fe-bearing phases. At a measurement temperature of 4.2 K, all Fe oxides have ordered into a sextet and the remaining ferric doublet represents Fe^{III} in clay minerals and/or in Fe–organic associations. The ferric doublets dominating the Mössbauer spectra obtained at room temperature (supporting information II) of the artificial soil incubated with and without straw addition completely ordered into sextets at 4.2 K (Fig. 4a), indicating that the artificial soil contained neither Fe^{III} in clay minerals nor in Fe–organic associations. In the artificial soil incubated without straw addition, the sextets mainly represent jarosite (95%), with small amounts of goethite (5%). No other Fe oxyhydroxides or Fe oxyhydroxy sulfate phases could be identified. After incubating the artificial soil with added straw, 16% of the initial total Fe were found in solution and 3% appeared as Fe^{2+} adsorbed on minerals or associated with OM (ferrous doublet in the

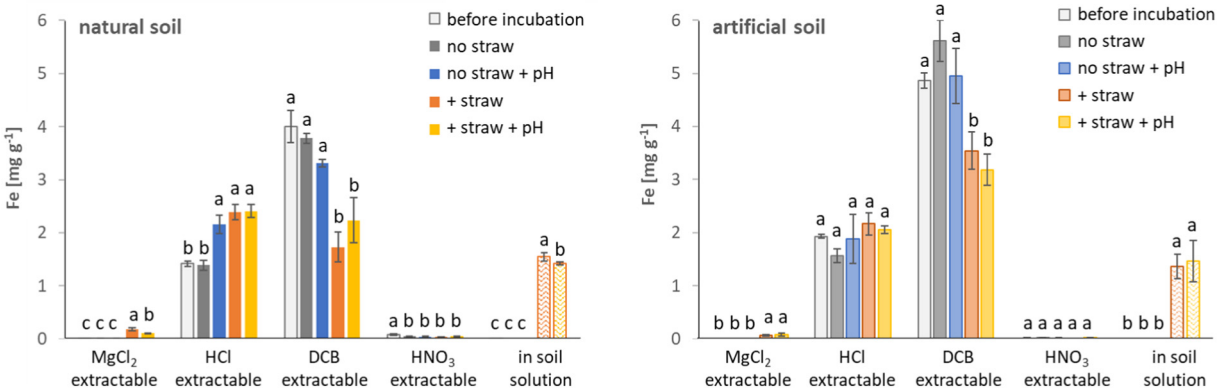

Fig. 3. Change of Fe fractions during incubation as revealed by sequential Fe extraction (bars show mean values ± standard deviation). Different letters indicate mean values significantly different between treatments ($p < 0.05$).

4.2 K spectrum; Winkler et al., 2018; Thompson et al., 2011). Seventy-one percent of the initial total Fe remained as jarosite (sharp sextet in the 4.2 K spectrum), while 9% of total Fe appeared as goethite, probably poorly crystalline or nano-sized (see broad sextet at room temperature and sextet in the 150 K spectrum (supporting information I and II). No evidence of any newly formed Fe sulfides was found.

In the natural soil incubated without straw addition, the prominent ferric doublet shown at room temperature (supporting information II) has mainly ordered into ferric sextets at 4.2 K, representing jarosite (85% of total Fe, Fig. 4b). There were no indications of any other Fe oxyhydroxy sulfate phases. Thirteen percent of total Fe, however, remained as ferric doublet at 4.2 K, thus representing Fe^{III} in phyllosilicates or Fe–organic associations. In natural soil incubated with straw addition, the ferric doublet ordered into a sharp sextet representing jarosite (23% of total Fe) and into a broad sextet, representing an unresolved jarosite-lepidocrocite phase (26% of total Fe). This is in contrast to the XRD result, which did not reveal the presence of jarosite in this sample. The ferric doublet remaining at 4.2 K accounts for 22% of total Fe, which was distinctly more than in the natural soil incubated without straw addition. Since formation of Fe^{III}-containing phyllosilicates is unlikely during a 15-week incubation experiment, that increase most likely represents Fe^{III} in Fe–organic associations. Nineteen percent of the initial total Fe in the natural soil was found in solution after incubation with straw addition. The room temperature Mössbauer spectra of the natural soil exhibited small ferrous doublets representing Fe^{II} in primary minerals or phyllosilicates or Fe^{2+} adsorbed on mineral surfaces or OM (supporting information II). That ferrous doublet accounted for 2% of total Fe in the natural soil incubated without straw addition and for 6% in the respective soil incubated with straw addition. In accordance with the increased amount of dissolved Fe^{2+} in the natural soil with straw addition (Table 3), the larger percentage of the ferrous doublet in that soil likely represents Fe^{2+} adsorbed on minerals or OM. Again, sulfidic Fe was not detected.

4. Discussion

4.1. pH adjustment did not support remediation of a sandy sulfuric soil after adding sufficient OC

The corresponding developments of pH and Eh values during incubation indicate that the artificial sulfuric soil served well as a model for the natural sulfuric soil. In both soils, the addition of wheat straw induced increases in pH to pH >6.0 (Fig. 1), almost independent of any initial pH adjustment. The Eh values decreased from ≥500 to ≤50 mV at the end of the incubation, indicating microbial reduction processes. This is supported by the OC consumption (Table 2): with straw, between 10 and 19% of the total soil OC was consumed during incubation, whereas without straw addition, the OC consumption was lower (approx. 6% of the soil OC in natural soil). Persistently high Eh (≥500 mV) and low pH values (pH ≤4.5) indicate that no proton-consuming microbial reduction occurred without straw addition. The results are in good agreement with a former study of Kölbl et al. (2019), showing that addition of OC as wheat straw resulted in rapid changes of redox and pH values, accompanied by significant CO_2 release

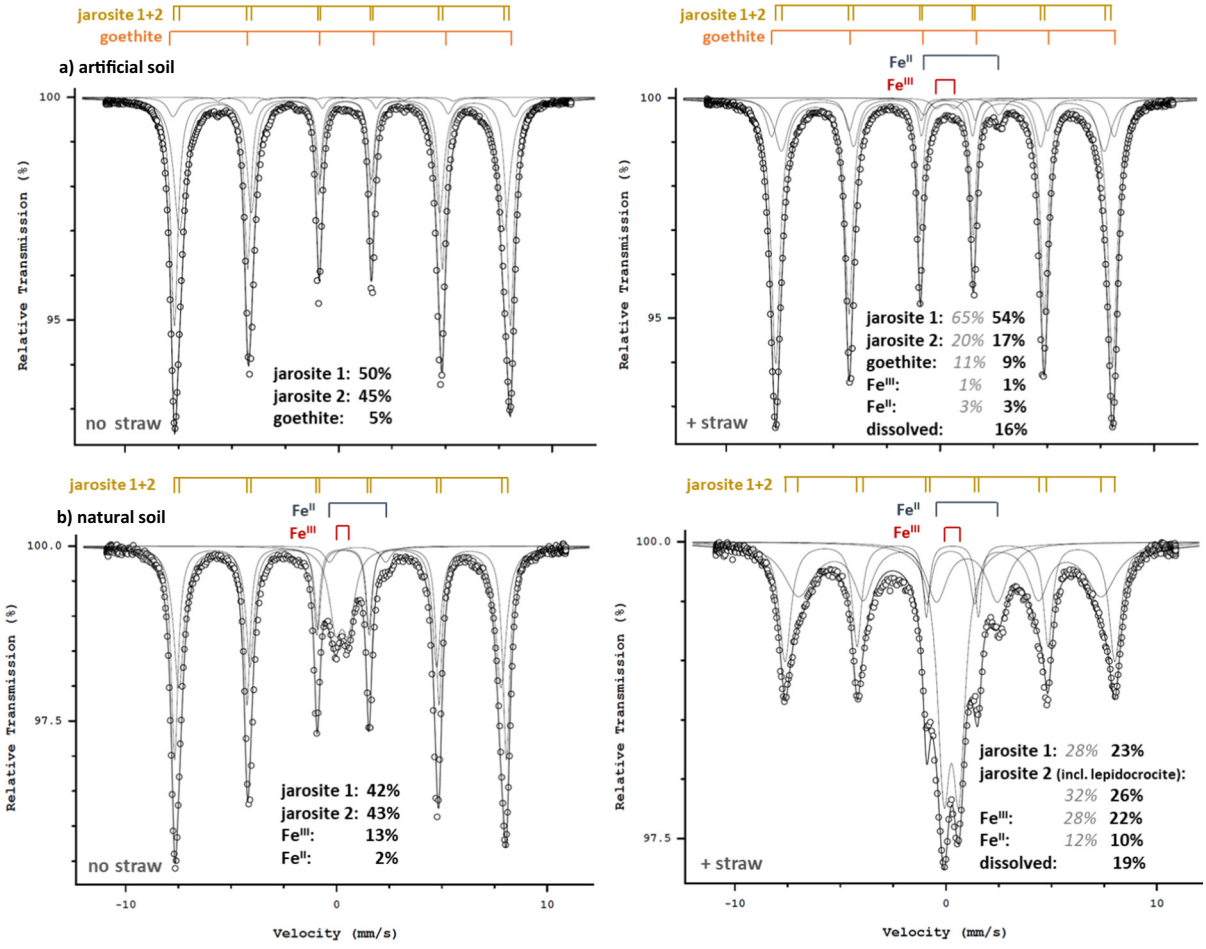

Fig. 4. Mössbauer spectra of artificial (a) and natural (b) soil treatments with and without straw addition (fine fractions) after incubation. Spectra were recorded at 4.2 K. Percentages given in grey italics reflect the Fe distribution after incubation with straw, but without taking into account the amount of dissolved Fe.

due to increased microbial activity and higher bacterial abundance than in treatments without straw addition.

The absence of recognizable effects of the prior pH adjustment on final pH and Eh values suggests that neutralization of acidity is not necessarily a prerequisite for the successful remediation of sandy sulfuric soils by submergence in combination with addition of available OM sources. This contrasts previous findings (e.g., Yuan et al., 2015a; Kölbl et al., 2018) that showed the effectiveness of combined pH plus OC treatments for remediation of clayey sulfuric soils. One possible explanation could be that the sandy sulfuric soil has less stored acidity than the clayey sulfuric soil. Another factor could be the amount of OC addition: It has not yet been tested whether there are different minimum levels of OC additions for different types of sulfuric soils that would make pH pre-adjustments unnecessary. Obviously, in this sandy sulfuric soil, microbial reduction processes proceed without pH adjustment, provided that added OC is sufficiently microbially available.

4.2. Redox processes caused by the addition of wheat straw induced dissolution of jarosite

The addition of wheat straw caused increased concentrations of Fe, K, and S in solution of natural and artificial soil samples (Table 3) and led to the complete loss of XRD-detectable jarosite in natural soil after incubation (Fig. 2). This could be due to microbially mediated reduction of jarosite as well as the pH increase. The stability of jarosite is limited to relatively oxidized (Eh >400 mV) and acid (pH 3–4) conditions and dissolution rates increase outside this range (Trueman et al., 2020; Keene et al., 2010; Gasharova et al., 2005; Baron and Palmer, 1996). Under inundation, Fe and/or sulfate-reducing bacteria can potentially utilize both Fe^{III} and SO_4^{2-} in jarosite as electron acceptors (Coggon et al., 2012), and thus, induce reductive dissolution (Chu et al., 2006). Such reductive dissolution increases not only the concentrations of Fe^{2+}, S, and K, but also the pH in the soil solution by proton-consuming reactions of reducing bacteria. In all treatments receiving straw, pH values ≥6 occurred over a period of at least 10 weeks during the incubation experiment. Since the stability of jarosite is generally limited to a narrow pH 3–4 range (Keene et al., 2010; Zahrai et al., 2013), the circumneutral pH likely contributed to the dissolution of jarosite. Thus, Fe^{3+}, K, and SO_4^{2-} are released into the soil solution due to dissolution of jarosite upon the increase in pH caused by reducing processes stimulated by organic substrate addition (Herzsprung et al., 2002; Bao et al., 2018).

The Fe, K, and S concentrations in solution did not reflect the stoichiometric composition of jarosite. In natural soil, the molar S:K ratio was greater than that of jarosite, indicating the occurrence of other sulfate minerals (such as gypsum or other S-bearing salts; Trueman et al., 2020), which were not present in the artificial soil. Instead of the expected molar Fe:K ratio of 3:1, we observed noticeably lower ratios in solution (Fe:K ratio ≤ 1.6:1) (Table 3), indicating precipitation of the released Fe in both natural and artificial soil. The Mössbauer data reveal that the dissolution of jarosite was accompanied by formation of secondary Fe oxyhydroxides (goethite, lepidocrocite; Fig. 4a, b), which will leave K and SO_4^{2-} in the solution. In addition, Mössbauer data show that released Fe^{3+} and Fe^{2+} may sorb on mineral surfaces, and the formation of Fe–organic associates (probably Fe—OM co-precipitates) is also likely to occur. High proportions of SO_4^{2-}-S to total S in the soil solution indicate that SO_4^{2-} reduction was little during 15 weeks anoxic incubation. This is supported by a former study showing that straw addition increased the total bacterial abundance, but not the proportion of SRB in the total bacterial community (Kölbl et al., 2019). On the one hand, this might be due to the energetic favourability of Fe^{III} versus SO_4^{2-} reduction (Burton et al., 2007). On the other hand, SRB prefer low-molecular weight organic compounds such as lactate, formate, and acetate (Holmer and Storkholm, 2001; Blodau, 2006), which were probably not sufficiently produced during straw decomposition by Fe-reducing bacteria. Therefore, formation of Fe sulfides appears unlikely as long as jarosite and other Fe^{III} forms are still present.

4.3. Reductive dissolution of jarosite does not immediately lead to formation of Fe sulfides

Jarosite was not detected by XRD in the natural soil after anoxic incubation with wheat straw but Mössbauer spectroscopy still revealed its presence. We hypothesize a decrease in crystal size and amount rendered jarosite undetectable by XRD. This is in accordance with studies using imaging techniques, which demonstrated reduction in grain size during alkaline dissolution of jarosite under oxic conditions (Gasharova et al., 2005; Smith et al., 2006). Also, substantial changes in jarosite morphology under reducing conditions via fragmentation from extensive etching and pitting (Vithana et al., 2015) may have contributed to decreased particle size.

Decreased particle size of jarosite would also explain the shift from dominating proportions of DCB-soluble Fe before incubation to higher proportions of HCl-soluble Fe after incubation with wheat straw (Fig. 3). According to Claff et al. (2010), loss of DCB-soluble Fe indicates loss of crystalline Fe oxide minerals, including jarosite. In turn, increasing proportions of HCl-soluble Fe are indicative of increasing amounts of labile metal sulfides (e.g., mackinawite, greigite), poorly crystalline or nano-sized oxyhydroxides, and labile organic—metal complexes (Yu et al., 2015).

Saturation indices (supporting information III) were calculated to estimate if Fe oxyhydroxides, Fe sulfides, and Fe oxyhydroxy sulfates are likely to dissolve or precipitate based on soil solution data. The results suggest thermodynamically favourable conditions for jarosite dissolution at the end of the incubations, even in the controls. However, jarosite solubility, excluding microbial-mediated reductive dissolution, is low at pH <4.5 (Trueman et al., 2020). The addition of OM accelerates the dissolution and increases Fe^{2+} concentrations in the solution, presumably via biotic Fe reduction. The improved conditions for jarosite dissolution, and thus, increased Fe concentrations at circumneutral pH and Eh between 0 and 50 mV in treatments with straw addition allow for precipitation of Fe oxyhydroxides but obviously not formation of Fe sulfides (supporting information III).

Mössbauer spectra confirmed jarosite losses after anoxic incubation with wheat straw (Fig. 4a,b), and revealed no formation of Fe sulfides. Instead, as predicted by the saturation indices, small amounts of probably poorly crystalline or nano-sized goethite were formed in the artificial soil, and lepidocrocite in the natural soil. Formation of goethite and lepidocrocite under anoxic conditions is well documented and has been attributed to Fe^{2+}-catalysed transformation of less crystalline Fe oxyhydroxides, such as ferrihydrite, to thermodynamically more stable forms (Williams and Scherer, 2004; Pedersen et al., 2005; Vogelsang et al., 2016; Karimian et al., 2018a, and references therein). Also, Fe oxyhydroxy sulfate phases undergo Fe^{2+}-catalysed transformation to goethite and lepidocrocite under anoxic conditions and cirumneutral pH (Burton et al., 2007; Jones et al., 2009; Vithana et al., 2015). Moreover, the formation of nano-sized goethite (diameters <100 nm) has also been shown as result of alkaline dissolution of jarosite under oxic conditions (Elwood Madden et al., 2012). Goethite crystals were observed both associated with the surfaces of jarosite grains as well as independent particles. Such nano-sized mineral phases are hardly detectable by XRD because they lack diffraction domains.

Vithana et al. (2015) showed that transformation of jarosite under anoxic conditions in re-flooded sediments led to the formation of goethite as well as lepidocrocite after 5 months of incubation. At low Eh values and high activity of microbial reducers, dissolution of jarosite could also promote the formation of Fe sulfides (Herzsprung et al., 2002). The formation of nanoparticulate mackinawite as described by Burton et al. (2007), however, only occurred after a biogeochemical regime shift from an initial dominance of Fe^{III} reduction to a co-occurrence of both Fe^{III} and SO_4^{2-} reduction, i.e. when reduction of Fe^{III} produced similar energy yields as SO_4^{2-} reduction. In our study, however, redox potentials between 0 and 50 mV and high proportions of SO_4^{2-} in the soil solution indicate that redox processes were mainly controlled by

the Fe^{II}–Fe^{III} redox couple, with little to no sulfate reduction, and therefore formation of Fe sulfides was not supported. The absence of Fe sulfide formation may also be the result of fast immobilization of released Fe^{2+} by sorption or co-precipitation with OM, as has been shown for estuarine sediments (Yu et al., 2015).

The formation of Fe oxyhydroxides instead of Fe sulfides has several implications and potential advantages for remediation of sulfuric soils and materials. In acid mine drainage and acid sulfate soil environments, potentially toxic trace elements, such as arsenic and antimony, can reside within the structure of jarosite and become released upon jarosite dissolution. However, neoformed lepidocrocite and goethite may immobilise these elements again, since they are strong scavengers for both at circumneutral pH conditions (Karimian et al., 2017; Karimian et al., 2018b). Thus, formation of lepidocrocite and goethite can reduce the risk of arsenic and antimony. Further, Fe oxyhydroxides, unlike Fe sulfides, are stable under oxic conditions and do not carry the risk of renewed acidification in the case of future aeration. Therefore, slow transformation of jarosite to Fe oxyhydroxides while avoiding sulfide formation is desirable. This could be achieved by moderate addition of OC, which favours the Fe^{II}–Fe^{III} redox couple, while avoiding sulfate-reducing conditions.

5. Conclusions

In contrast to previous studies and in contrast to our original expectation, pH pre-adjustment was neither necessary for anoxic remediation of the natural sandy sulfuric soil nor for its artificial analogue. As hypothesized, sufficient addition of straw induced reduction processes that consumed protons, leading to increased pH values and the dissolution of jarosite. In contrast to our assumptions, high proportions of SO_4^{2-} in the soil solution indicate that SO_4^{2-} reduction was negligible during the 15-week incubation under submerged conditions. Consequently, and in contrast to our original assumption, formation of Fe sulfides did not take place. Instead, we observed formation of nano-sized goethite (in artificial soil), lepidocrocite (in natural soil), as well as Fe^{2+}/Fe^{3+} either sorbed to minerals or associated with OM. Since Fe oxyhydroxides, unlike Fe sulfides, are not prone to support renewed acidification in the case of future aeration, this result has important implications for the remediation of sulfuric soils. We suggest addition of OC at amounts that maintain redox conditions allowing transformation from jarosite to Fe oxyhydroxides while avoiding sulfide formation.

CRediT authorship contribution statement

Angelika Kölbl: Conceptualization, Methodology, Investigation, Writing – original draft. **Klaus Kaiser:** Conceptualization, Investigation, Writing – review & editing. **Pauline Winkler:** Writing – review & editing. **Luke Mosley:** Writing – review & editing. **Rob Fitzpatrick:** Writing – review & editing. **Petra Marschner:** Writing – review & editing. **Friedrich E. Wagner:** Investigation. **Werner Häusler:** Investigation. **Robert Mikutta:** Writing – review & editing.

Declaration of competing interest

The authors declare that they have no known competing financial interests or personal relationships that could have appeared to influence the work reported in this paper.

Acknowledgements

We thank Anja Kroner and Alexandra Boritzki for sample preparation and laboratory analyses. Prof. Dr. Dr. Herbert Pöllmann and Jacqueline Wassmann (Institute of Geosciences and Geography) are greatfully acknowledged for providing glove box access and conducting sulfate analyses, respectively. The study was funded by Deutsche Forschungsgemeinschaft (DFG), project "Interactions between organic matter and iron oxyhydroxysulfates / iron sulfides during remediation of acid sulfate soils" (KO 2245/3-2). LM and RF would like to acknowledge the contribution of Australian Research Council Discovery Project funding to this research (DP170104541).

Appendix A. Supplementary data

Supplementary data to this article can be found online at https://doi.org/10.1016/j.scitotenv.2021.145546.

References

Bao, Y.P., Guo, C.L., Lu, G.N., Yi, X.Y., Wang, H., Dang, Z., 2018. Role of microbial activity in Fe(III) hydroxysulfate mineral transformations in an acid mine drainage-impacted site from the Dabaoshan mine. Sci. Total Environ. 616, 647–657.
Baron, D., Palmer, C.D., 1996. Solubility of jarosite at 4-35 degrees C. Geochim. Cosmochim. Acta 60, 185–195.
Berner, R.A., 1984. Sedimentary pyrite formation: an update. Geochim. Cosmochim. Acta 48, 605–615.
Blodau, C., 2006. A review of acidity generation and consumption in acidic coal mine lakes and their watersheds. Sci. Total Environ. 369, 307–332.
Burton, E.D., Bush, R.T., Sullivan, L.A., Mitchell, D.R.G., 2007. Reductive transformation of iron and sulfur in schwertmannite-rich accumulations associated with acidified coastal lowlands. Geochim. Cosmochim. Acta 71, 4456–4473.
Chu, C.X., Lin, C.X., Wu, Y.G., Lu, W.Z., Long, J., 2006. Organic matter increases jarosite dissolution in acid sulfate soils under inundation conditions. Aust. J. Soil Res. 44, 11–16.
Claff, S.R., Sullivan, L.A., Burton, E.D., Bush, R.T., 2010. A sequential extraction procedure for acid sulfate soils: partitioning of iron. Geoderma 155, 224–230.
Coggon, M., Becerra, C.A., Nüsslein, K., Miller, K., Yuretich, R., Ergas, S.J., 2012. Bioavailability of jarosite for stimulating acid mine drainage attenuation. Geochim. Cosmochim. Acta 78, 65–76.
dos Santos Afonso, M.D., Stumm, W., 1992. Reductive dissolution of iron(III) (hydr)oxide by hydrogen sulfide. Langmuir 8, 1671–1675.
Driscoll, R.L., Leinz, R.W., 2005. Methods for synthesis of some jarosites. In: U.S.G.S.T.a.M. (Ed.), 5-D1. U.S. Geological Survey, Reston, Virginia.
Elwood Madden, M.E., Madden, A.S., Rimstidt, J.D., Zahrai, S., Kendall, M.R., Miller, M.A., 2012. Jarosite dissolution rates and nanoscale mineralogy. Geochim. Cosmochim. Acta 91, 306–321.
Fanning, D.S., Rabenhorst, M.C., Fitzpatrick, R.W., 2017. Historical developments in the understanding of acid sulfate soils. Geoderma 308, 191–206.
Fitzpatrick, R.W., 2013. Demands on soil classification and soil survey strategies: Special-purpose soil classification Systems for Local Practical use. In: Shahid, S., Taha, F., Abdelfattah, M. (Eds.), Developments in Soil Classification, Land Use Planning and Policy Implications: Innovative Thinking of Soil Inventory for Land Use Planning and Management of Land Resources. Springer, Dordrecht, pp. 51–83.
Fitzpatrick, R.W., Thomas B.P., Merry R.H., Marvanek, S., 2012. A field guide to estuarine soil-landscapes in barker inlet, South Australia. Acid sulfate soils Centre, the University of Adelaide. Report ASSC_005. 50 pp. https://www.adelaide.edu.au/directory/robert.fitzpatrick?dsn=directory.file;field=data;id=40576;m=view.
Gasharova, B., Göttlicher, J., Becker, U., 2005. Dissolution at the surface of jarosite: an in situ AFM study. Chem. Geol. 215, 499–516.
Herzsprung, P., Friese, K., Frömmichen, R., Göttlicher, J., Koschorreck, M., Tümpling, W.V., Wendt-Potthoff, K., 2002. Chemical changes in sediment pore-waters of an acidic mining lake after addition of organic substrate and lime for stimulating lake remediation. Water Air Soil Pollut.: Focus 2, 123–140.
Holmer, M., Storkholm, P., 2001. Sulphate reduction and Sulphur cycling in lake sediments: a review. Freshw. Biol. 46, 431–451.
Isbell, R.F., National Committee on Soils and Terrain, 2016. The Australian Soil Classification, Second Edition. CSIRO Publishing, Clayton, Victoria, Australia (R.F. Isbell: The Australian Soil Classification, CSIRO Publishing, Melbourne, Australia).
IUSS Working Group WRB. 2015. World Reference Base for soil resources 2014, update 2015. International soil classification system for naming soils and creating legends for soil maps. World soil resources reports no. 106. FAO, Rome.
Jayalath, N., Fitzpatrick, R.W., Mosley, L., Marschner, P., 2016a. Type of organic carbon amendment influences pH changes in acid sulfate soils in flooded and dry conditions. J. Soils Sediments 16, 518–526.
Jayalath, N., Mosley, L.M., Fitzpatrick, R.W., Marschner, P., 2016b. Addition of organic matter influences pH changes in reduced and oxidised acid sulfate soils. Geoderma 262, 125–132.
Johnston, S.G., Keene, A.F., Bush, R.T., Burton, E.D., Sullivan, L.A., Smith, D., McElnea, A.E., Martens, M.A., Wilbraharn, S., 2009. Contemporary pedogenesis of severely degraded tropical acid sulfate soils after introduction of regular tidal inundation. Geoderma 149, 335–346.
Johnston, S.G., Burton, E.D., Keene, A.F., Planer-Friedrich, B., Voegelin, A., Blackford, M.G., Lumpkin, G.R., 2012. Arsenic mobilization and iron transformations during sulfidization of As(V)-bearing jarosite. Chem. Geol. 334, 9–24.
Jones, A.M., Collins, R.N., Rose, J., Waite, T.D., 2009. The effect of silica and natural organic matter on the Fe(II)-catalysed transformation and reactivity of Fe(III) minerals. Geochim. Cosmochim. Acta 73, 4409–4422.
Karimian, N., Johnston, S.G., Burton, E.D., 2017. Antimony and arsenic behavior during Fe (II)-induced transformation of jarosite. Environ. Sci. Technol. 51, 4259–4268.
Karimian, N., Johnston, S.G., Burton, E.D., 2018a. Iron and sulfur cycling in acid sulfate soil wetlands under dynamic redox conditions: a review. Chemosphere 197, 803–816.

Karimian, N., Johnston, S.G., Burton, E.D., 2018b. Antimony and arsenic partitioning during Fe2+-induced transformation of jarosite under acidic conditions. Chemosphere 195, 515–523.
Keene, A., Johnston, S., Bush, R., Sullivan, L., Burton, E., 2010. Reductive dissolution of natural jarosite in a tidally inundated acid sulfate soil: geochemical implications. 19th World Congress of Soil Science, Soil Solutions for a Changing World 1–6 August 2010, Brisbane, Australia, pp.100–103.
Kölbl, A., Marschner, P., Mosley, L., Fitzpatrick, R., Kögel-Knabner, I., 2018. Alteration of organic matter during remediation of acid sulfate soils. Geoderma 332, 121–134.
Kölbl, A., Bucka, F., Marschner, P., Mosley, L., Fitzpatrick, R., Schulz, S., Lueders, T., Kögel-Knabner, I., 2019. Consumption and alteration of different organic matter sources during remediation of a sandy sulfuric soil. Geoderma 347, 220–232.
Lovley, D.R., 1995. Microbial reduction of iron manganese, and other metals. Adv. Agron. 54, 175–231.
Mehra, O.P., Jackson, M.L., 1960. Iron oxide removal from soils and clays by a dithionite–citrate system buffered with sodium bicarbonate. Clay Clay Miner. 7, 317–327.
Michael, P.S., Fitzpatrick, R., Reid, R., 2015. The role of organic matter in ameliorating acid sulfate soils with sulfuric horizons. Geoderma 255, 42–49.
Pedersen, H.D., Postma, D., Jakobsen, R., Larsen, O., 2005. Fast transformation of iron oxyhydroxides by the catalytic action of aqueous Fe(II). Geochim. Cosmochim. Acta 69, 3967–3977.
Plugge, C.M., Zhang, W., Scholten, J.C.M., Stams, A.J.M., 2011. Metabolic flexibility of sulfate-reducing bacteria. Front. Microbiol. 2, 81.
Poch, R.M., Thomas, B.P., Fitzpatrick, R.W., Merry, R.H., 2009. Micromorphological evidence for mineral weathering pathways in a coastal acid sulfate soil sequence with Mediterranean-type climate, South Australia. Aust. J. Soil Res. 47, 403–422.
Smith, A.M.L., Hudson-Edwards, K.A., Dubbin, W.E., Wright, K., 2006. Dissolution of jarosite [$KFe_3(SO_4)_2(OH)_6$] at pH 2 and 8: insights from batch experiments and computational modelling. Geochim. Cosmochim. Acta 70, 608–621.
Stirling, E., Fitzpatrick, R., Mosley, L.M., 2020. Drought effects on wet soils in inland wetlands and peatlands. Earth-Sci. Rev. 210, 103387.
Stookey, L.L., 1970. Ferrozine - a new spectrophotometric reagent for iron. Anal. Chem. 42, 779–781.
Thompson, A., Rancourt, D.G., Chadwick, O.A., Chorover, J., 2011. Iron solid-phase differentiation along a redox gradient in basaltic soils. Geochim. Cosmochim. Acta 75, 119–133.
Trueman, A.M., McLaughlin, M.J., Mosley, L.M., Fitzpatrick, R.W., 2020. Composition and dissolution kinetics of jarosite-rich segregations extracted from an acid sulfate soil with sulfuric material. Chem. Geol. 543, 119606.
Vithana, C.L., Sullivan, L.A., Burton, E.D., Bush, R.T., 2015. Stability of schwertmannite and jarosite in an acidic landscape: prolonged field incubation. Geoderma 239, 47–57.
Vogelsang, V., Fiedler, S., Jahn, R., Kaiser, K., 2016. In-situ transformation of iron-bearing minerals in marshland-derived paddy subsoil. Eur. J. Soil Sci. 67, 676–685.
Welch, S.A., Christy, A.G., Kirste, D., Beavis, S.G., Beavis, F., 2007. Jarosite dissolution I - trace cation flux in acid sulfate soils. Chem. Geol. 245, 183–197.
Williams, A.G.B., Scherer, M.M., 2004. Spectroscopic evidence for Fe(II)−Fe(III) electron transfer at the iron oxide−water interface. Environ. Sci. Technol. 38, 4782–4790.
Winkler, P., Kaiser, K., Thompson, A., Kalbitz, K., Fiedler, S., Jahn, R., 2018. Contrasting evolution of iron phase composition in soils exposed to redox fluctuations. Geochim. Cosmochim. Acta 235, 89–102.
Yu, C.X., Virtasalo, J.J., Karlsson, T., Peltola, P., Osterholm, P., Burton, E.D., Arppe, L., Hogmalm, J.K., Ojala, A.E.K., Astrom, M.E., 2015. Iron behavior in a northern estuary: large pools of non-sulfidized Fe(II) associated with organic matter. Chem. Geol. 413, 73–85.
Yuan, C.L., Fitzpatrick, R., Mosley, L.M., Marschner, P., 2015a. Sulfate reduction in sulfuric material after re-flooding: effectiveness of organic carbon addition and pH increase depends on soil properties. J. Hazard. Mater. 298, 138–145.
Yuan, C.L., Mosley, L., Fitzpatrick, R., Marschner, P., 2015b. Amount of organic matter required to induce sulfate reduction in sulfuric material after re-flooding is affected by soil nitrate concentration. J. Environ. Manag. 151, 437–442.
Zahrai, S.K., Madden, M.E.E., Madden, A.S., Rimstidt, J.D., 2013. Na-jarosite dissolution rates: the effect of mineral composition on jarosite lifetimes. Icarus 223, 438–443.